Table S1. Intercomparison of applied statistical measures (*BIAS, IOA, r, RMSE, NMSEunsys, NMSEsys*) with minimum, median and maximum values, between measured $(\overline{PM_{10}})_d$ (310 rural background stations from Airbase) and modelled $(\overline{PM_{10}})_d$ with the WRF-Chem and EMEP models during November 2011 with respect to the station height (same as Fig 8).

		WRF-Chem			EMEP		
	Height	**MIN**	**MEDIAN**	**MAX**	**MIN**	**MEDIAN**	**MAX**
BIAS	Sea-level	-86	-44	2	-68	-26	47
	Elevated	-91	-55	100	-80	-29	132
	Mountain	-91	-33	196	-76	13	226
IOA	Sea-level	0.4	0.9	1.0	0.7	0.9	1.0
	Elevated	0.3	0.8	1.0	0.5	0.9	1.0
	Mountain	0.4	0.8	1.0	0.6	0.9	1.0
R	Sea-level	0.02	0.39	0.87	0.02	0.48	0.87
	Elevated	0.00	0.21	0.88	0.00	0.28	0.85
	Mountain	0.01	0.19	0.82	0.00	0.24	0.75
RMSE	Sea-level	6.9	20.7	60.8	5.0	17.3	50.2
	Elevated	4.2	19.6	114.7	3.5	15.8	111.0
	Mountain	2.2	12.7	36.6	3.0	13.2	34.0
NMSEsys	Sea-level	0.0	0.3	5.5	0.0	0.1	1.4
	Elevated	0.0	0.7	9.3	0.0	0.2	3.3
	Mountain	0.0	0.3	9.4	0.0	0.2	2.4
NMSEunsys	Sea-level	-0.7	0.4	1.7	-0.3	0.3	0.9
	Elevated	0.0	0.5	1.9	0.1	0.3	1.6
	Mountain	0.2	0.7	2.4	0.1	0.4	1.5

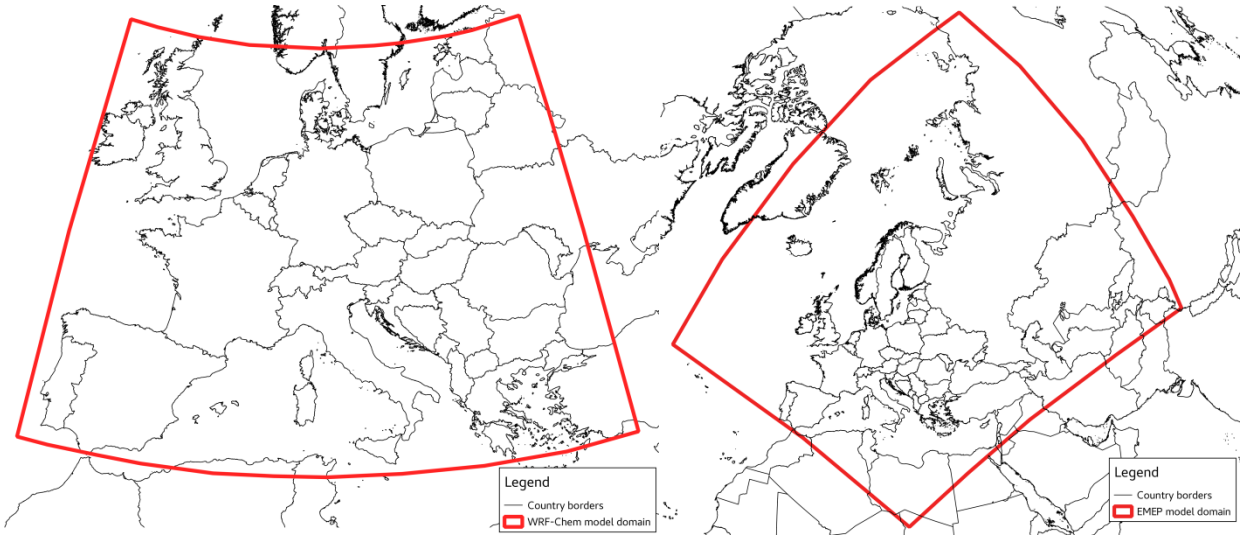

Figure S1. WRF-Chem (left) and EMEP (right) model domains.

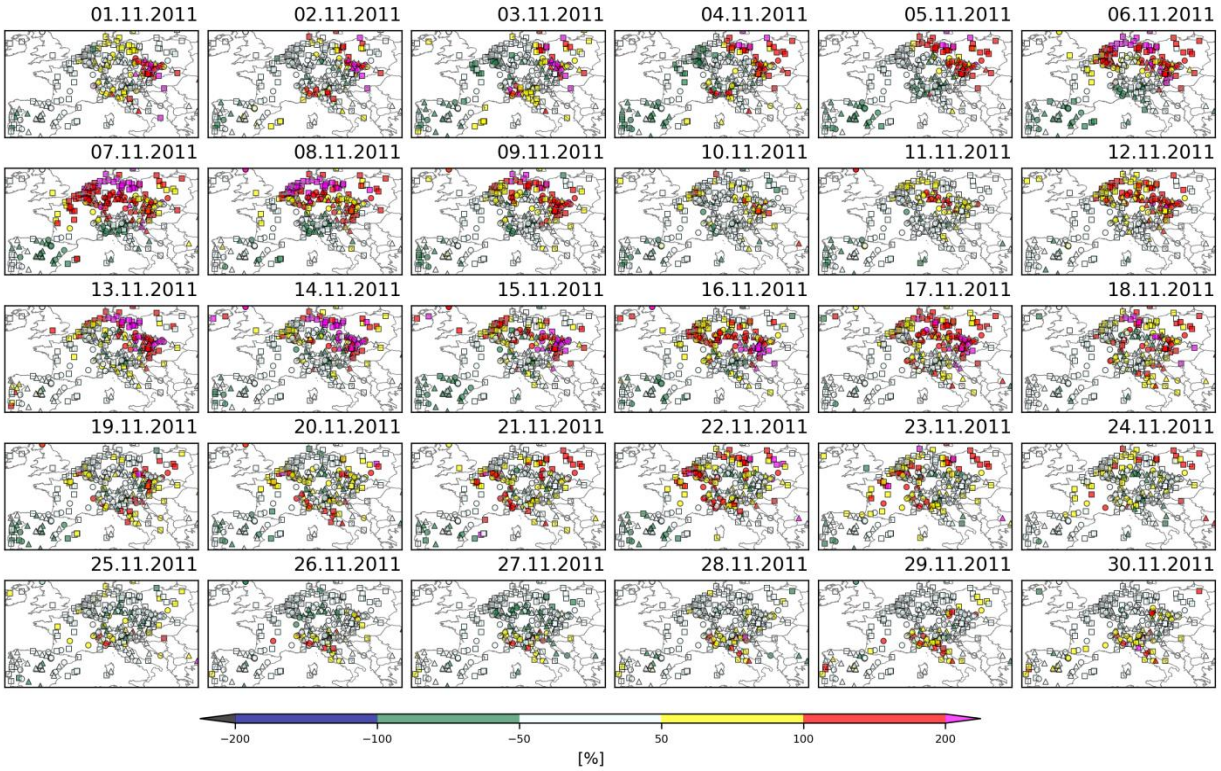

Figure S2. The difference (DF) between $(\overline{PM_{10}})_d$ and $(\overline{PM_{10}})_a$concentrations (equation 9) over Europe during November 2011.

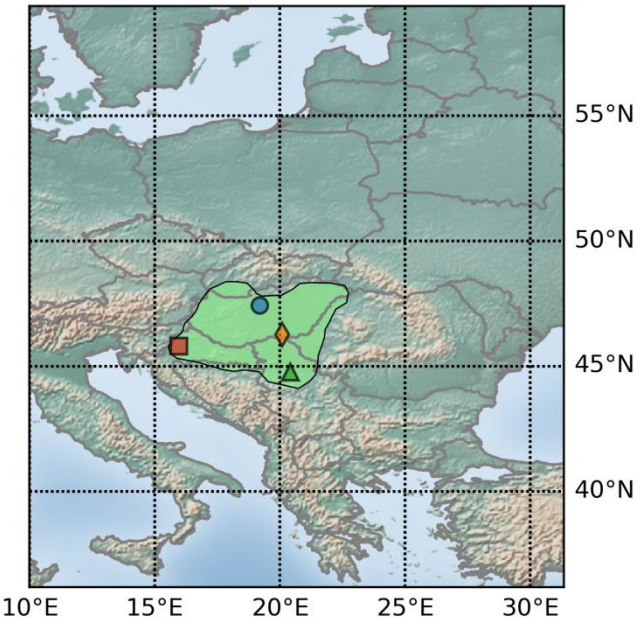

Figure S3. Pannonian basin (green area) with the location of measurement stations ▲ – Belgrade, ● – Budapest, ♦ - Szeged, ■ – Zagreb.

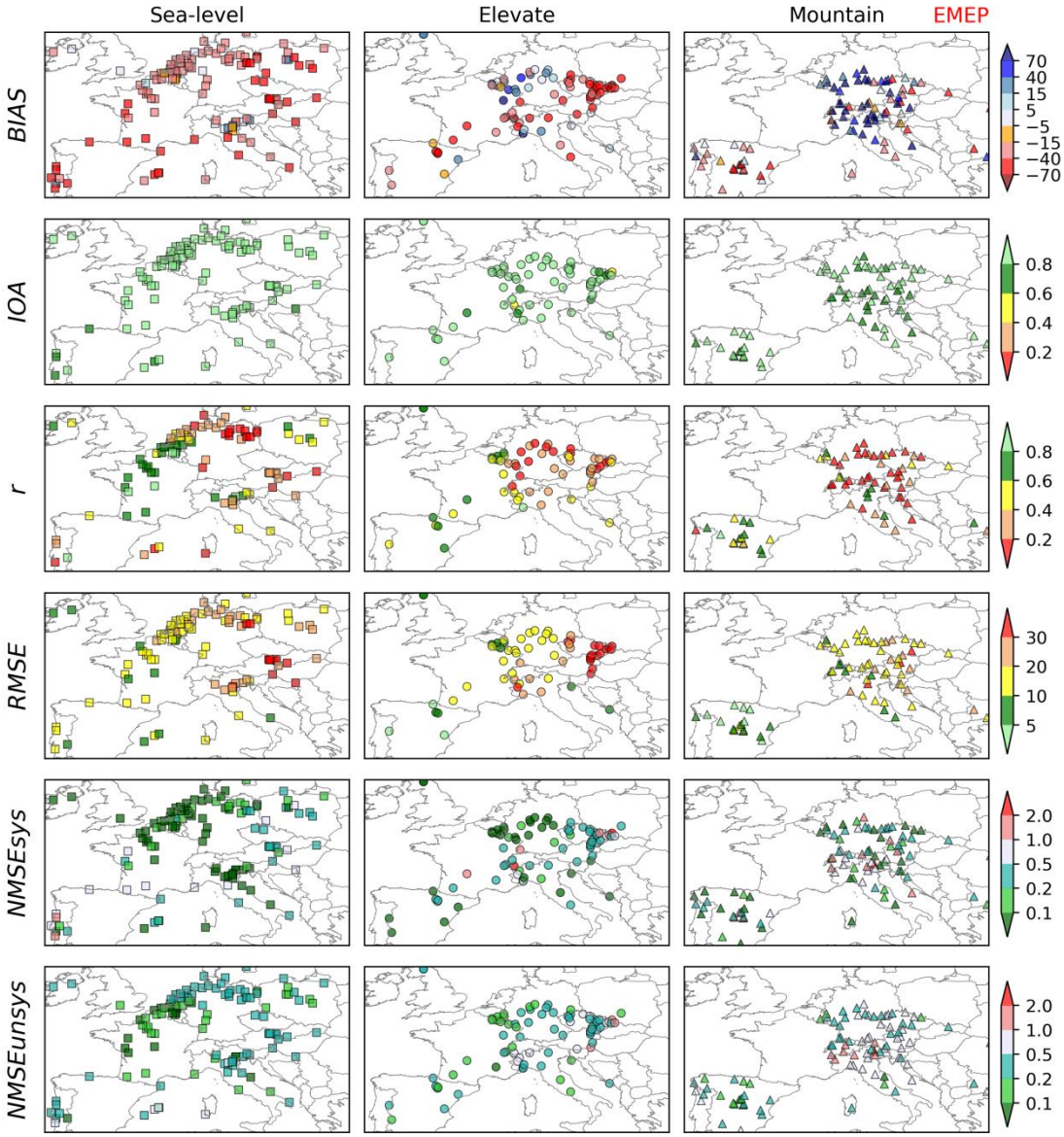

Figure S4. Comparison of statistical parameters between measured $(\overline{PM_{10}})_d$ (Airbase) and modelled $(\overline{PM_{10}})_d$ with the EMEP model during a one-month period (November 2011) with respect to the station height: *BIAS*, *IOA*, *r*, *RMSE*, *NMSEunsys*, *NMSEsys*.

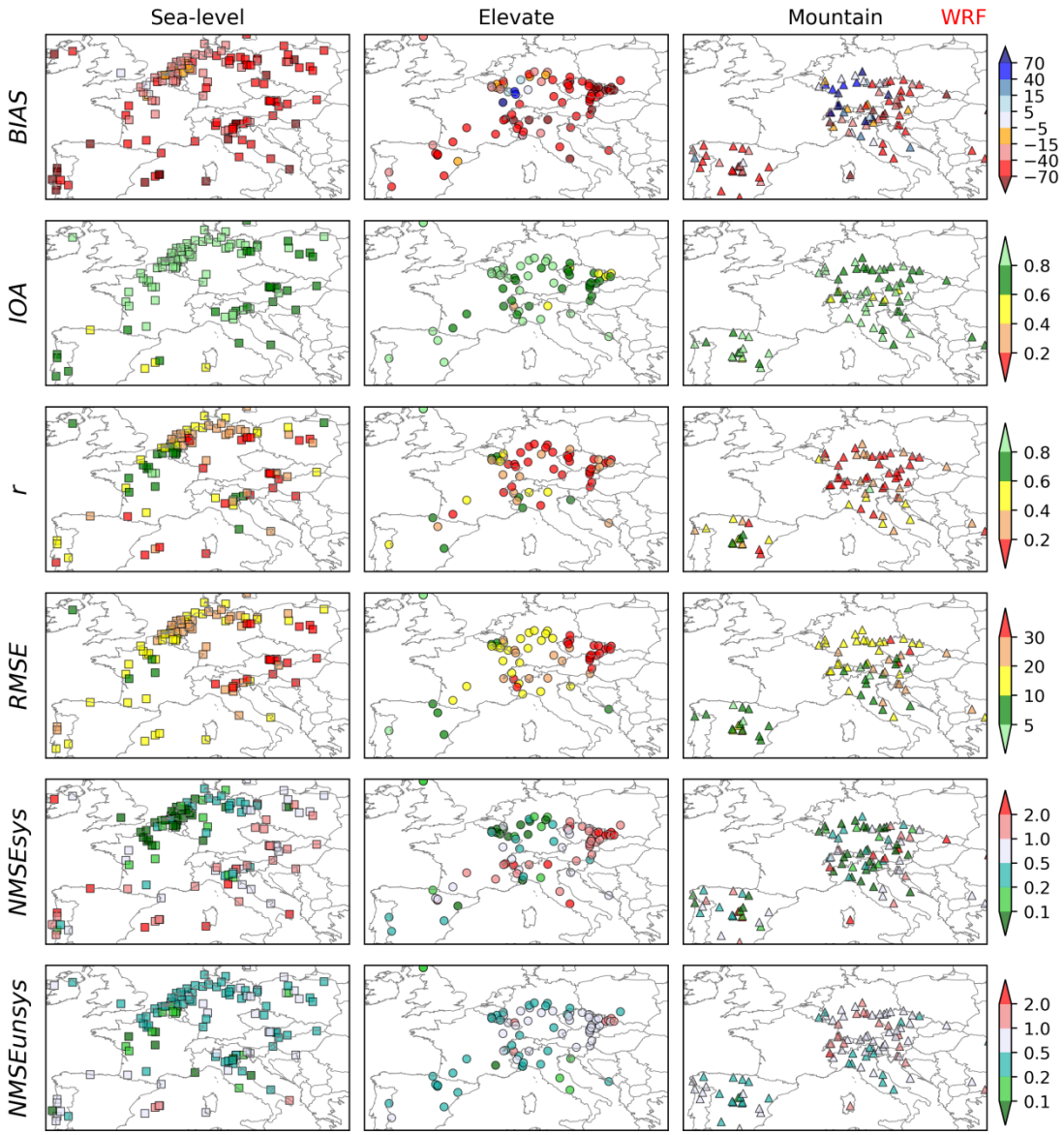

Figure S5. Comparison of the statistical parameters between measured $(\overline{PM_{10}})_d$ concentrations (*Airbase*) and modelled $(\overline{PM_{10}})_d$ with the WRF-Chem model during a one-month period (November 2011) with respect to the station height: *BIAS*, *IOA*, *r*, *RMSE*, *NMSEunsys*, *NMSEsys*.

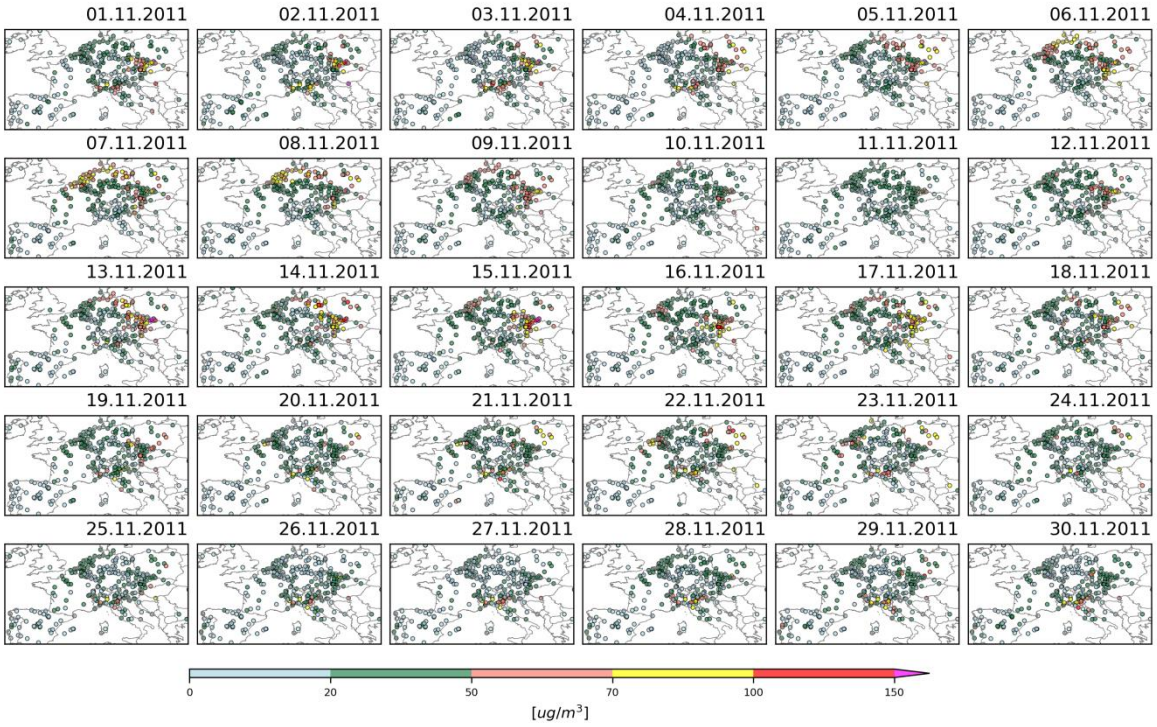

Figure S6. $(\overline{PM_{10}})_d$ for all rural background stations within the domain during November 2011.

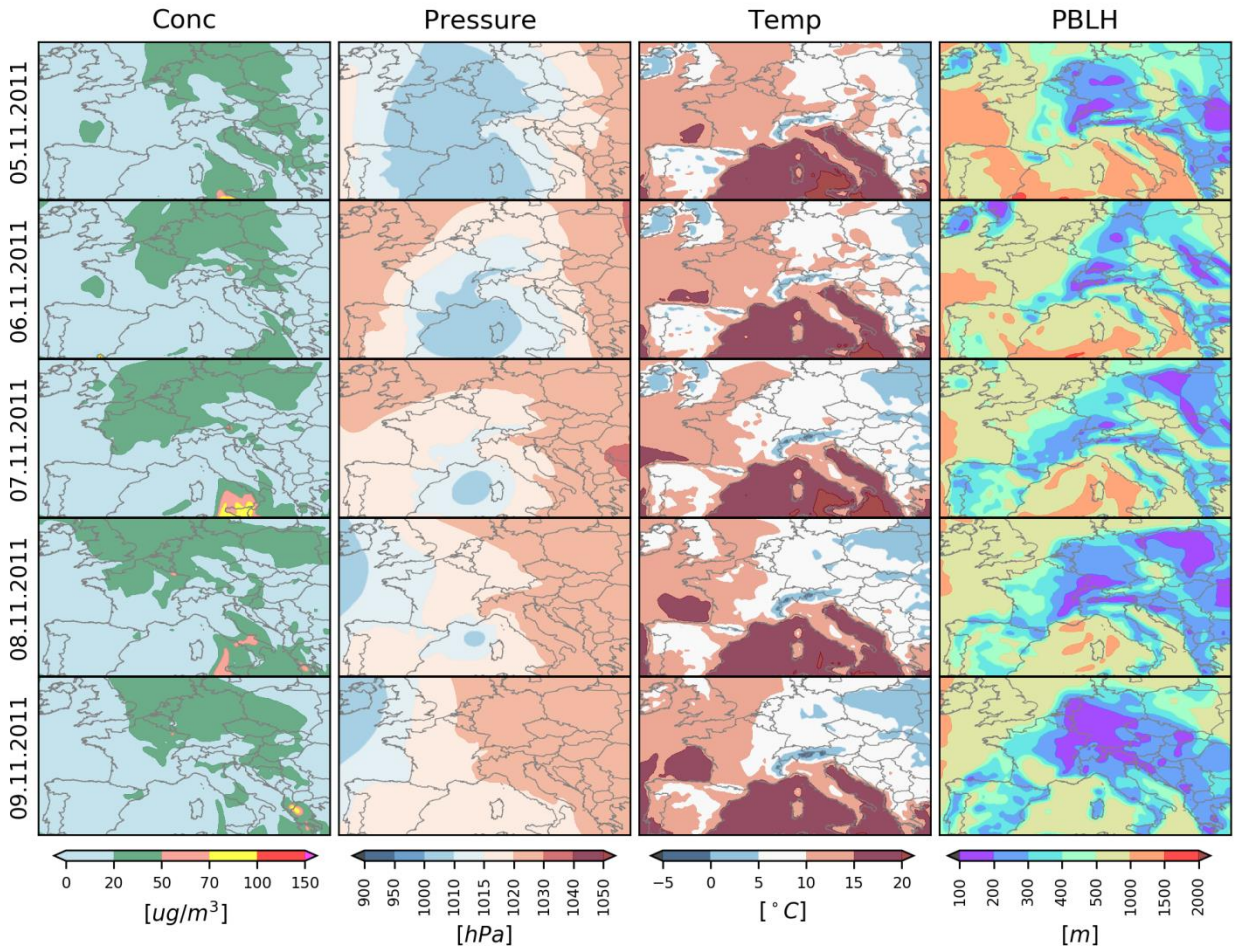

Figure S7. Modelled $(\overline{PM_{10}})_d$ as *Conc*, and $\left(\overline{mslp}\right)_d$ as *Pressure*, $(\overline{t_{2m}})_d$ as *Temp* and $\left(\overline{pblh}\right)_d$ as *PBLH* during the first high pollution episode (the EMEP model)**.**

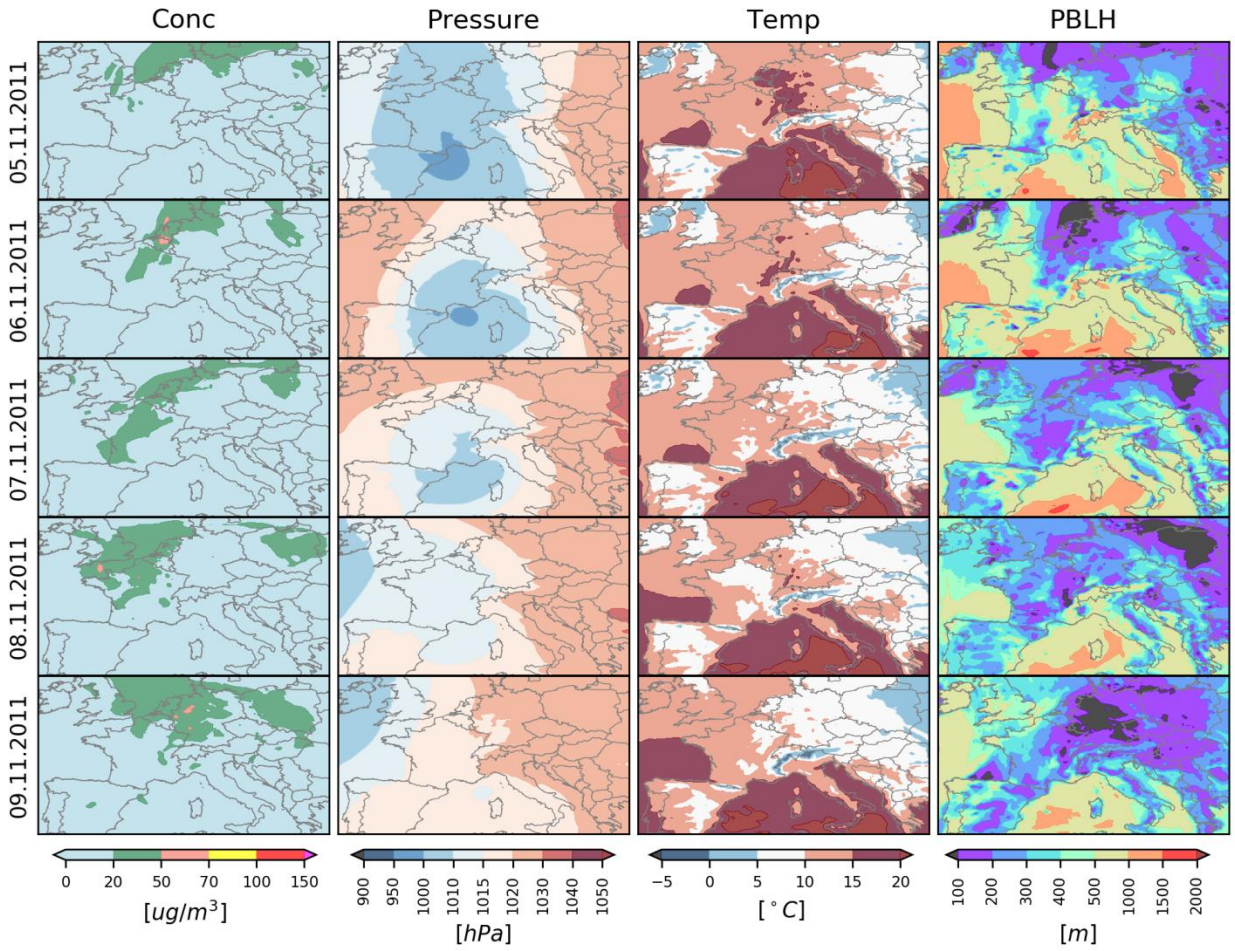

Figure S8. Same as Fig S4 but for the WRF-Chem model.

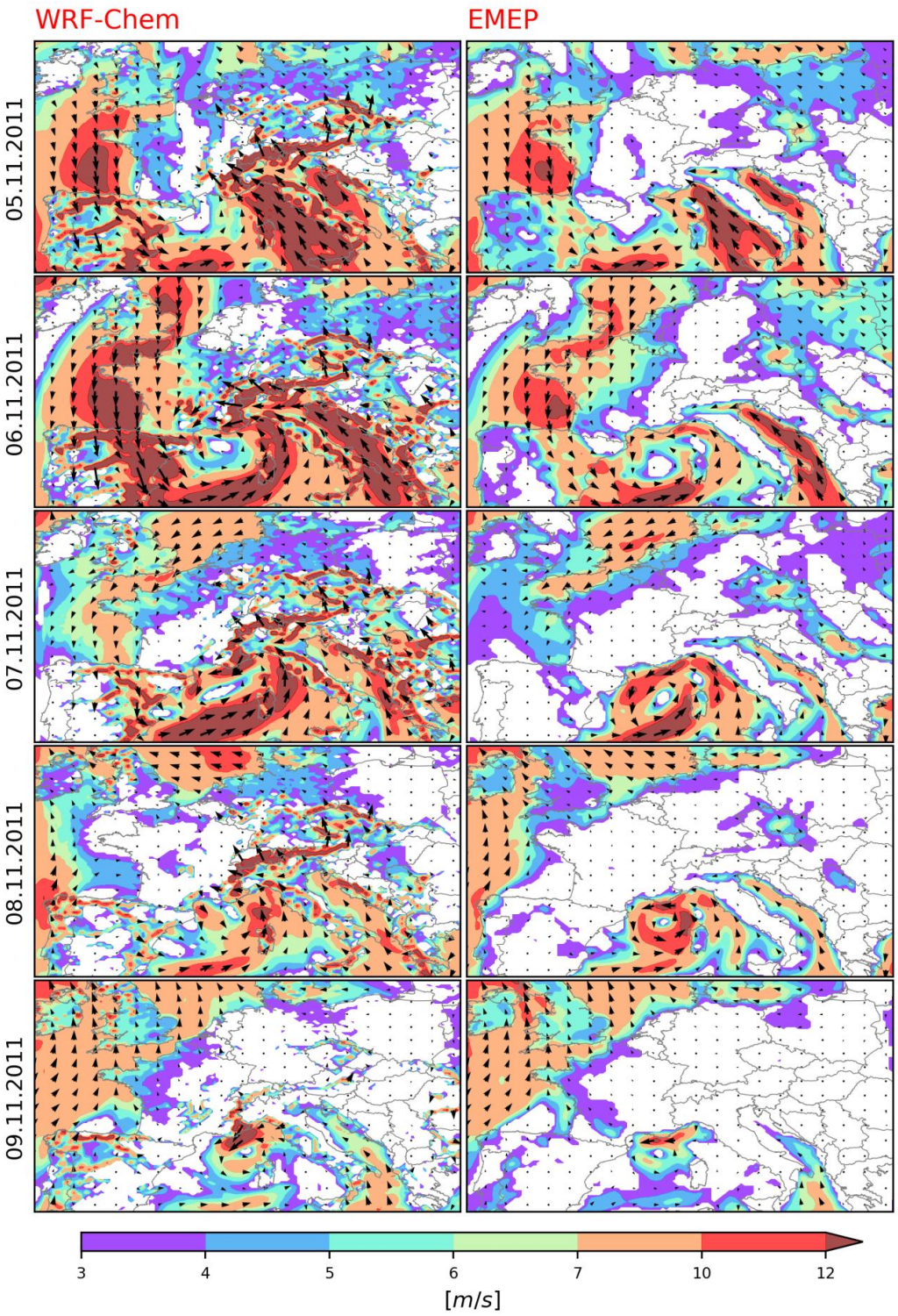

Figure S9 Modelled daily averaged wind speed and direction during the first high pollution episode for the WRF-Chem (left) and EMEP models (right).

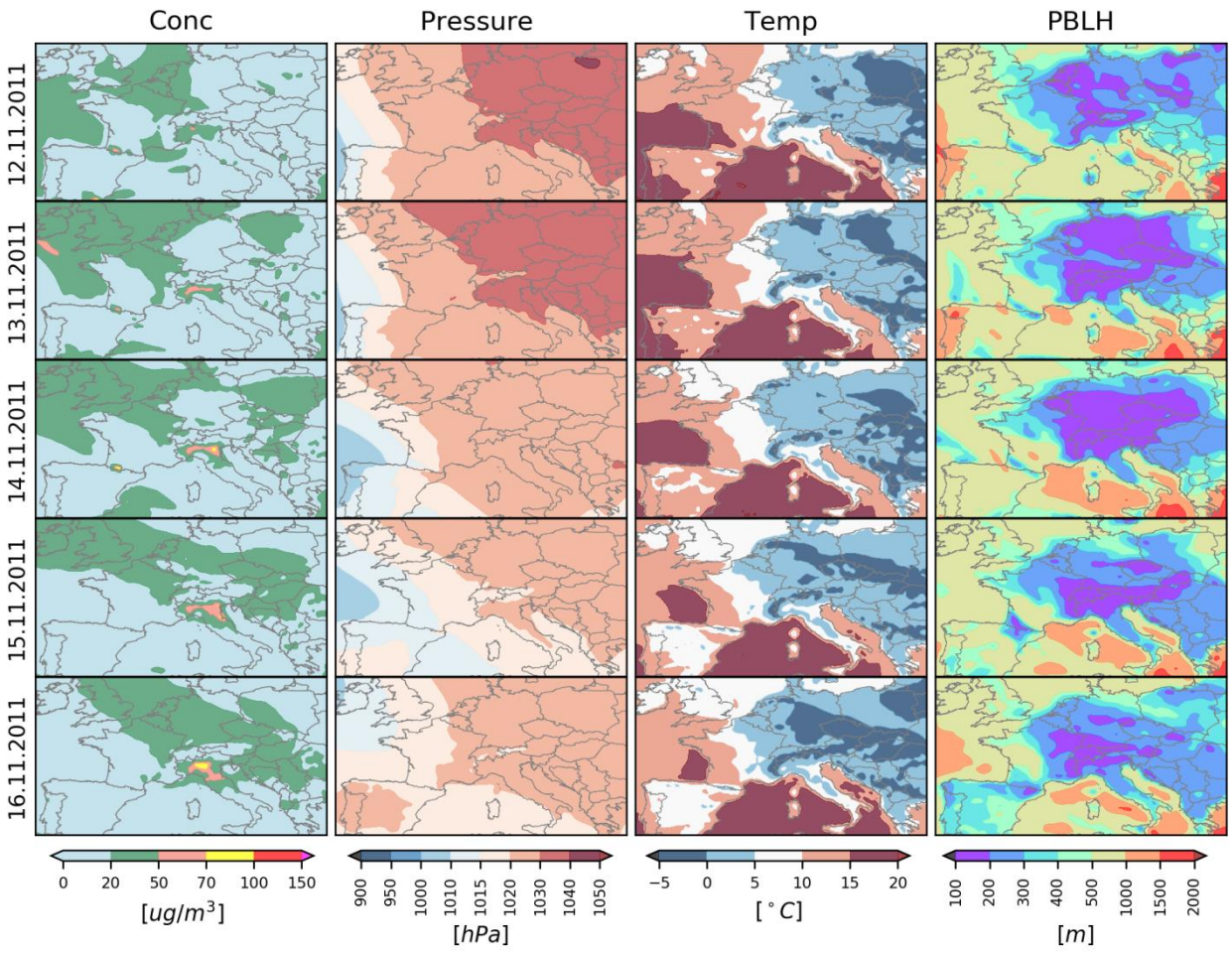

Figure S10. Modelled $(\overline{PM_{10}})_d$ as *Conc*, and $\left(\overline{mslp}\right)_d$ as *Pressure*, $(\overline{t_{2m}})_d$ as *Temp* and $\left(\overline{pblh}\right)_d$ as *PBLH* during the second high pollution episode (the EMEP model).

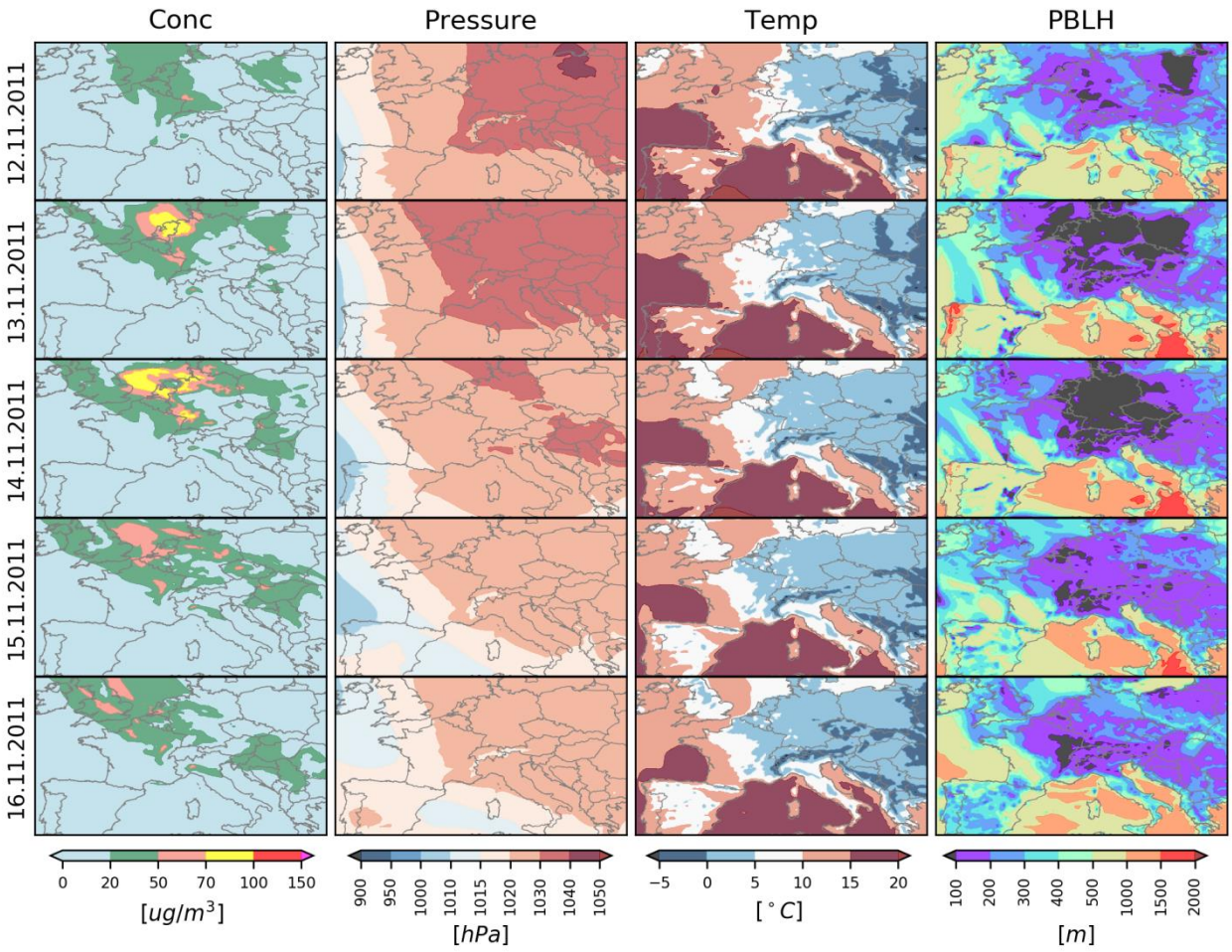

Figure S11. Same as Fig S4 but for the WRF-Chem model.

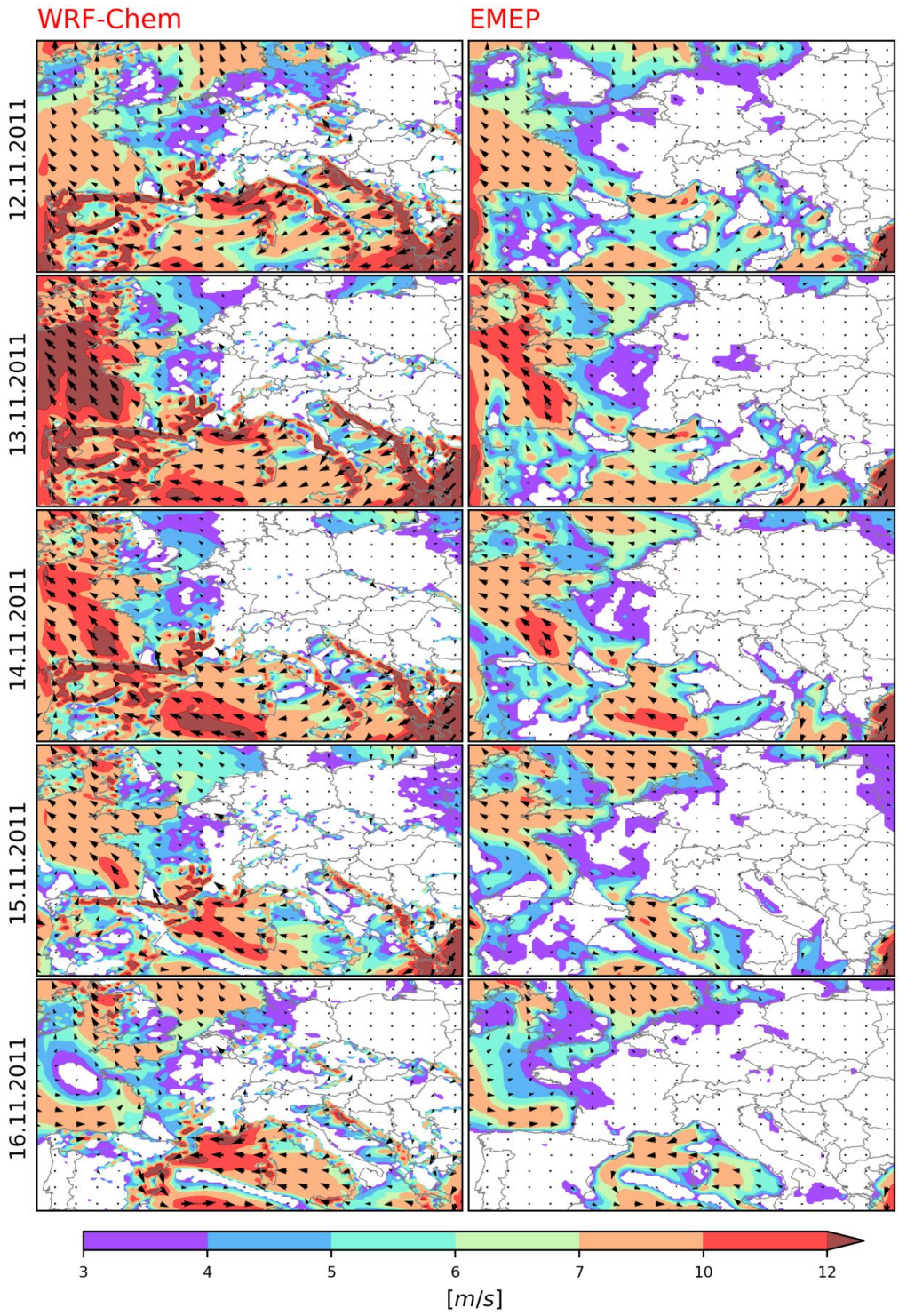

Figure S12. Modelled daily averaged wind speed and direction during the first high pollution episode for the WRF-Chem (left) and EMEP models (right).

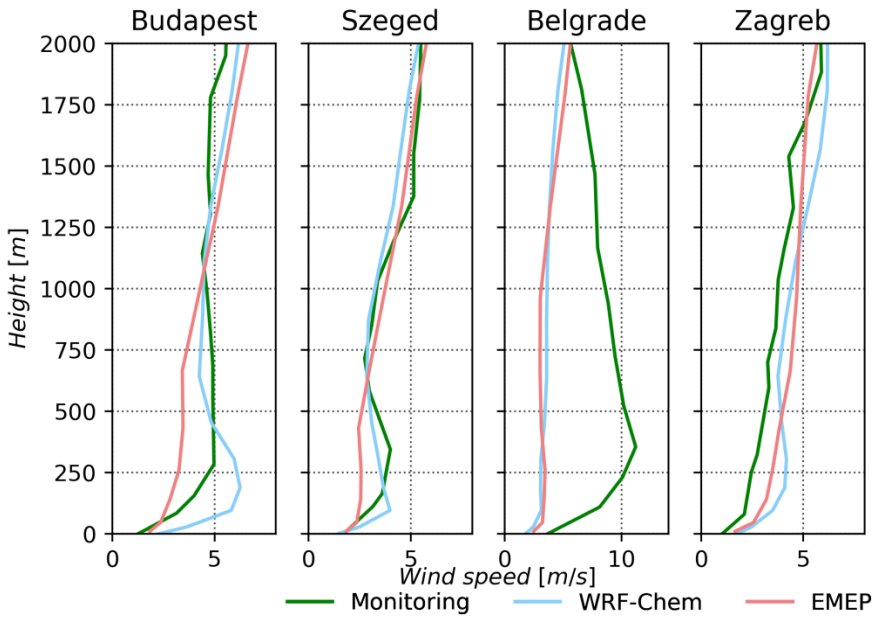

Figure S13. Comparison of the modelled averaged vertical profile for wind speed and soundings up to 2 km during the second high pollution episode.